Characterization of trichromatic color cameras by using a new multispectral imaging technique

Vien Cheung and Stephen Westland

School of Design University of Leeds, Leeds, LS2 9JT, UK

Changjun Li

Colour Chemistry Department University of Leeds, Leeds, LS2 9JT, UK

Jon Hardeberg and David Connah

Department of Computer Science and Media Technology Gjøvik University College, 2802 Gjøvik, Norway

We investigate methods for the recovery of reflectance spectra from the responses of trichromatic camera systems and the application of these methods to the problem of camera characterization. The recovery of reflectance from colorimetric data is an ill-posed problem, and a unique solution requires additional constraints. We introduce a novel method for reflectance recovery that finds the smoothest spectrum consistent with both the colorimetric data and a linear model of reflectance. Four multispectral methods were tested using data from a real trichromatic camera system. The new method gave the lowest maximum colorimetric error in terms of camera characterization with test data that were independent of the training data. However, the average colorimetric performances of the four multispectral methods were statistically indistinguishable from each other but were significantly worse than conventional methods for camera characterization such as polynomial transforms. © 2005 Optical Society of America

OCIS codes: 330.1690, 330.1730, 120.5700, 110.6980.

1. INTRODUCTION

A common approach to obtain device-independent color information from digital cameras is to characterize the device in terms of CIE tristimulus values.[1–7] Theoretically, the spectral sensitivities of a color-imaging system should satisfy the Luther condition by which they are a linear transformation of the CIE color-matching functions.[8] However, since the spectral sensitivities of most commercial color cameras do not satisfy the Luther condition owing to limitations of the manufacturing process, device metamerism may occur. Thus two spectrally different surfaces imaged under the same illumination may give rise to identical camera *RGB* responses (and identical *XYZ* values when the *RGB* values are transformed with a characterization model) and yet may not be a visual match when viewed in that illumination. Such device metamerism may seriously limit the colorimetric applications of characterized camera systems. In addition, the CIE tristimulus values obtained from the camera characterization are illuminant dependent.

In a multispectral imaging system the aim is to recover the spectral information of the samples being imaged.[9–12] Such an approach, if successful, would effectively convert the camera into an imaging spectrophotometer and would ultimately permit the measurement of device- and illuminant-independent images. Multispectral imaging is possible because the spectral properties of most surfaces are relatively smooth functions of wavelength.[13] If the reflectance spectra of surfaces were less constrained, then it would not be possible to recover them completely (or even approximately to any reasonable degree) from the responses of a relatively small number of channels.

Recently some researchers have suggested that multispectral imaging, or spectral techniques more generally, may be useful for the characterization of imaging devices such as cameras and scanners.[5,14,15] A possible device-characterization method is to try to recover the spectral properties of the surfaces in the scene from the camera responses and then compute the tristimulus values from the estimated reflectances.[5] This paper addresses the question of whether such spectral-based characterization methods can outperform conventional characterization methods. The approach taken is to capture the camera responses of a number of surfaces for which the spectral reflectance values (and the tristimulus values) are known and to compute estimated tristimulus values from spectral data derived from the camera responses to these surfaces by using multispectral techniques.

In this study three previously published multispectral techniques are considered and their effectiveness for camera characterization evaluated. A new technique for recovering spectral information is introduced and compared with the existing techniques. The colorimetric accuracy of the multispectral techniques are compared with some previously published performance data by using conventional characterization techniques based on the same camera and samples.[16]

2. REFLECTANCE-RECOVERY METHODS

Some basic nomenclature is first introduced before the reflectance-recovery methods are described in detail. Many multispectral-imaging techniques exploit the inherent smoothness of reflectance spectra with the use of low-dimensional linear models.[9] Thus a reflectance $P(\lambda)$ sampled at equal intervals of wavelength λ may be approximated by a weighted sum of m basis functions $B_i(\lambda)$ with $i \in 1 \ldots m$ so that (in matrix notation)

$$\mathbf{P} = \mathbf{BW}, \tag{1}$$

where, if we assume that spectral properties are sampled at 31 wavelength intervals, $\mathbf{P}$ is a $31 \times n$ matrix of reflectance values that represent n reflectance spectra, $\mathbf{W}$ is a $m \times n$ matrix of weights, and $\mathbf{B}$ is a $31 \times m$ matrix of basis functions so that column i contains the ith basis function $B_i(\lambda)$. Column j of the matrix $\mathbf{W}$ contains m scalars that provide an efficient representation of the jth reflectance spectrum.

A. Maloney–Wandell Method
The method proposed by Maloney and Wandell[17] assumes a linear camera model represented by Eq. (2),

$$\mathbf{C} = \mathbf{M}^T\mathbf{P}, \tag{2}$$

where $\mathbf{C}$ is a $3 \times n$ matrix of camera responses and $\mathbf{M}$ is a 31×3 matrix that contains wavelength-by-wavelength product of the spectral sensitivity of the camera and the spectral power distribution of the light source. If the linear-model representation of reflectance [Eq. (1) is substituted into Eq. (2)], then

$$\mathbf{C} = \mathbf{\Lambda W}, \tag{3}$$

where the $3 \times m$ matrix $\mathbf{\Lambda}$ represents the product $\mathbf{M}^T\mathbf{B}$ and $\mathbf{M}^T$ represents the transpose of $\mathbf{M}$. The surface-reflectance factors may be recovered by manipulating Eq. (3) to yield

$$\mathbf{W} = \mathbf{\Lambda}^+\mathbf{C}, \tag{4}$$

where $\mathbf{\Lambda}^+$ denotes the pseudoinverse of the matrix $\mathbf{\Lambda}$ that is known if the spectral sensitivities of the camera's channels, the spectral power of the illuminant, and the spectral properties of the basis functions are all known. Once the weight matrix $\mathbf{W}$ is computed [from Eq. (4)], it is then trivial to compute the reflectance from Eq. (1).

B. Imai–Berns Method
Imai and Berns developed a method for reflectance recovery based directly on Eq. (3) in which the system matrix $\mathbf{\Lambda}$ is empirically determined by a least-squares analysis.[18] For the Maloney–Wandell method it is necessary to determine the space of basis functions in which the reflectance spectra will be represented, to measure the spectral power distribution of the light source, and to determine the spectral sensitivities of the imaging system. The Imai–Berns method, however, requires only the first of these steps: the determination of the basis functions. The value of $\mathbf{\Lambda}$ is then found directly by optimization.

Equation (3) may be manipulated to yield an expression to compute $\mathbf{\Lambda}$ thus,

$$\mathbf{\Lambda} = \mathbf{CW}^+, \tag{5}$$

where $\mathbf{W}^+$ denotes the pseudoinverse of the matrix $\mathbf{W}$. Once $\mathbf{\Lambda}$ is determined, Eqs. (1) and (4) may be used to recover the reflectance from the camera responses.

C. Shi–Healey Method
The Maloney–Wandell and Imai–Berns methods each use a linear model of reflectance to constrain the possible solutions to the problem of finding a reflectance spectrum given a set of camera responses. Low-dimensional linear models of reflectance are usually used with these methods so that the dimensionality of the reflectance model is less than or equal to the number of camera channels.[11,18] Since this study is concerned with trichromatic imaging systems, the number of basis functions should be three or less in the Maloney–Wandell and Imai–Berns methods. Alternative ways to constrain the solution have been proposed that may be better suited to the use of higher-than-three-dimensional models of reflectance. For example, in the method proposed by Shi and Healey,[15] Eq. (1) may be expanded to give

$$\mathbf{P} = \mathbf{B}_1\mathbf{W}_1 + \mathbf{B}_2\mathbf{W}_2, \tag{6}$$

where $\mathbf{B}_1$ contains the first three basis functions (assuming three channels in the camera), $\mathbf{B}_2$ contains the remaining basis functions, and $\mathbf{W}_1$ and $\mathbf{W}_2$ are the respective weight vectors for the matrix of reflectance spectra $\mathbf{P}$. Equation (6) can be substituted into Eq. (2) to give

$$\mathbf{C} = \mathbf{M}^T\mathbf{B}_1\mathbf{W}_1 + \mathbf{M}^T\mathbf{B}_2\mathbf{W}_2. \tag{7}$$

Left multiplying both sides of Eq. (7) by $(\mathbf{M}^T\mathbf{B}_1)^{-1}$ and rearranging produces an equation that expresses $\mathbf{W}_1$ in terms of $\mathbf{W}_2$ thus:

$$\mathbf{W}_1 = (\mathbf{M}^T\mathbf{B}_1)^{-1}\mathbf{C} - (\mathbf{M}^T\mathbf{B}_1)^{-1}\mathbf{M}^T\mathbf{B}_2\mathbf{W}_2. \tag{8}$$

We can now substitute Eq. (8) into Eq. (6) to give

$$\mathbf{P} = \mathbf{B}_1((\mathbf{M}^T\mathbf{B}_1)^{-1}\mathbf{C} - (\mathbf{M}^T\mathbf{B}_1)^{-1}\mathbf{M}^T\mathbf{B}_2\mathbf{W}_2) + \mathbf{B}_2\mathbf{W}_2, \tag{9}$$

which shows that the constraint provided by the $3 \times n$ matrix $\mathbf{C}$ reduces the number of degrees of freedom for $\mathbf{P}$ to $m - 3$. By varying the $m - 3$ degrees of freedom in $\mathbf{W}_2$, Shi and Healey find a set of reflectance spectra $\mathbf{P}$ that are consistent with the sensor responses $\mathbf{C}$ and the linear model of reflectance.

In Eq. (9) all of the components are known except for the vector $\mathbf{W}_2$. We can rearrange Eq. (9) to produce Eq. (10),

$$\mathbf{P} = \mathbf{B}_1(\mathbf{M}^T\mathbf{B}_1)^{-1}\mathbf{C} + (\mathbf{B}_2 - \mathbf{B}_1(\mathbf{M}^T\mathbf{B}_1)^{-1}\mathbf{M}^T\mathbf{B}_2)\mathbf{W}_2, \tag{10}$$

from which it is now clear that we have an expression for $\mathbf{P}$ in the form $\mathbf{AW}_2 + \mathbf{B}$ where $\mathbf{B} = \mathbf{B}_1(\mathbf{M}^T\mathbf{B}_1)^{-1}\mathbf{C}$ and $\mathbf{A} = (\mathbf{B}_2 - \mathbf{B}_1(\mathbf{M}^T\mathbf{B}_1)^{-1}\mathbf{M}^T\mathbf{B}_2)$, and $\mathbf{W}_2$ is the unknown. This form of equation can be solved with use of various constraints.

For simplicity, if we consider the solution of Eq. (10) for the 3×1 camera response $\mathbf{c}$ to a single reflectance spectrum, the solution proposed by Shi and Healey can be expressed as finding the 31×1 vector $\mathbf{p}$ that is as close as possible to a 31×1 reflectance vector $\mathbf{v}$ from a predeter-

mined characterization set of spectra.[15] In other words, a solution is found that is close to one of the spectra from the characterization set. In this case $\|\mathbf{p}-\mathbf{v}\|^2$ is minimized, or for the case of multiple spectra, $\|\mathbf{AW}_2+(\mathbf{B}-\mathbf{V})\|^2$ is minimized.

D. Li–Luo Method

Li and Luo[19] described a method of spectral recovery that was motivated by earlier work by van Trigt.[20,21] In this method van Trigt's smoothness condition, to find a single member of a metamer set[22] that satisfies a colorimetric constraint, was replaced by the square of two-norm of a vector. In a new method, which we term the Li–Luo method, the smoothness constraint has been used as an alternative way to solve Eq. (10). Thus the Li–Luo method uses the constraint that $\mathbf{p}$ must be smooth by minimizing $\|\mathbf{Qp}\|^2$, where $\mathbf{Q}$ is an operator that calculates the gradient of $\mathbf{p}$ at each point. Thus for a set of spectra, $\|\mathbf{Q}(\mathbf{AW}_2+\mathbf{B})\|^2$ is minimized. Constrained linear optimization is used to enforce the constraint $1 \geqslant \mathbf{p} \geqslant 0$.

3. EXPERIMENT

An experiment was conducted to evaluate the performance of four multispectral methods for camera characterization. The four methods are described in Section 2 and are referred to as the Maloney–Wandell, Imai–Berns, Shi–Healey, and Li–Luo methods.

An Agfa digital StudioCam camera, a three-chip CCD device with 8-bit resolution for each channel and 4500×3648 pixel spatial resolution, was used in this study. During the experiment the automatic white-balance setting of the camera was disabled. Three imaging targets, the Macbeth ColorChecker and ColorChecker DC charts and 50 color samples selected from the Natural Color System (NCS) were used for characterization. The spectral reflectance factors of the patches on each of the charts were measured by using an X-Rite 938 spectrodensitometer.

A. Measurement of Light Source

A Minolta CS1000 spectroradiometer was used for the measurement of the spectral power distribution of the lighting system (with nominal output corresponding to CIE illuminant D50), which consisted of two fluorescent tubes arranged approximately in a 45/0 illumination/viewing geometry. The spectroradiometer gave spectral information between 380 and 780 nm at 1-nm intervals, and a subsampling procedure was performed to convert the spectral data into 31 equally spaced samples between 400 and 700 nm. This allowed the calculation of CIE tristimulus values for the samples under the exact lighting conditions of the camera. The CIE chromaticity coordinates of the light source were 0.3559 and 0.3629 for the 1964 (10-deg) CIE observer.

B. Linearization and Spatial Correction

During the experiment the camera and lighting positions were fixed, and the *RGB* values of the Macbeth ColorChecker DC achromatic samples were measured with each in the center of the camera's field of view. Each patch generated an image region of about 18×18 pixels, but the

values of a central subregion (11×11 pixels) were averaged to generate the mean *RGB* values for that patch. For the achromatic samples there was little variation in the *RGB* values within the 11×11 subregions (the standard error of the mean was never greater than 0.22 RGB unit, and even for the darkest samples the standard deviation was less than 1%).

The camera *RGB* responses were measured for the achromatic samples from the Macbeth ColorChecker DC chart, an NCS uniform white paper, and the dark condition (with the camera lens cap in place) to allow a correction for any nonlinearity of the response of the camera (thus the raw camera responses were converted to values that were linearly related to the camera input). For each camera channel, a second-order polynomial was used to fit the relationship between the raw camera responses (normalized in the range 0–1) and the luminance reflectance factors (also normalized in the range 0–1) for the achromatic patches. The luminance reflectance factors (Y) were computed for each sample under the actual light source that was used to illuminate the samples during imaging. (Strictly speaking, the linearization should be carried with respect to the inputs to the channels,— obtained from the spectral reflectance factors of the sample, the spectral power distribution of the illumination, and the spectral sensitivities of the channels— rather than with respect to the normalized Y values.[23] However, the errors that result from using the luminous efficiency function as an estimate of the channel responses are negligible, given that the spectral reflectance factors of the achromatic samples on which the linearization is based are almost wavelength invariant.[24])

The three plots on the left-hand side of Fig. 1 show the normalized raw R (upper plot), G (middle plot), and B (lower plot) values for the gray samples plotted against the respective normalized measured luminance reflectance factors. The solid line in each panel shows the polynomial fit to the data, and since a high-quality camera is being used, it is evident that the correction for nonlinearity is tiny. However, these polynomial functions were used to subsequently convert all raw camera responses to linearized camera responses before further processing. The three plots on the right-hand side of Fig. 1 show the normalized linearized R (upper plot), G (middle plot), and B (lower plot) values for the achromatic samples plotted against the normalized measured luminance reflectance factors for those samples. A comparison of the left- and right-hand plots shows that a consequence of the linearization process is that a balancing of the channels is carried out. The R and B values for the white sample were $\sim$0.6 (corresponding to an 8-bit value of $\sim$150), whereas the maximum value of the G channel was $\sim$0.9. Following the linearization process, however, the right-hand plots illustrate that the maximum value of each of the channels is $\sim$0.8, thus correcting for any color cast from the combination of the illumination and the camera spectral sensitivity.

Spatial correction, according to a method previously used by Hardeberg[9] and later by Sun and Fairchild,[25] was also performed to minimize the effect of any spatial nonuniformity of the intensity of the illumination or of the sensitivity of the camera CCD array. For example, for the
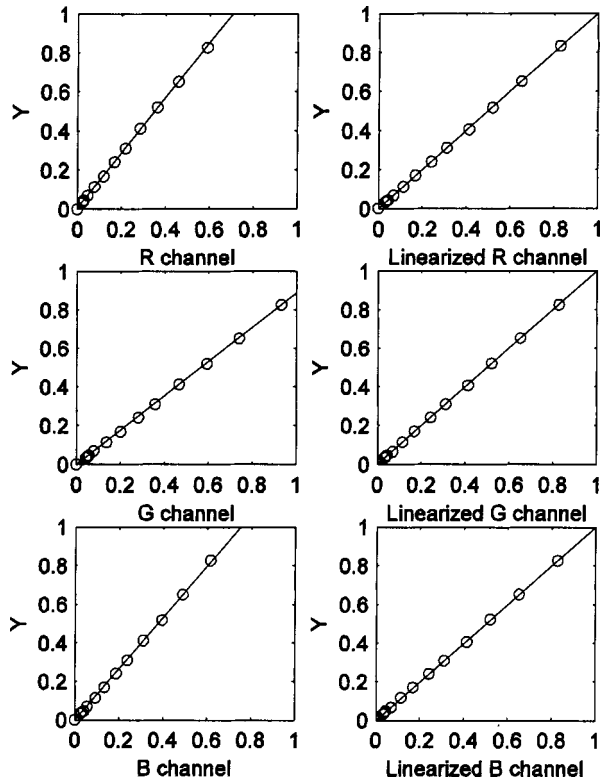
Fig. 1.   Luminance reflectance factors (Y) of 13 achromatic patches plotted against the spatially averaged camera channel *RGB* responses (circles) for each patch and third-order polynomial fit (solid lines) (left column) and the linearized camera responses (circles) converted from the polynomial fit (right column). The circles in the right-column graphs should lie along the straight line if the linearization process is perfect. All data are shown normalized in the range 0–1.

red channel, Eq. (11) was used to convert the linearized channel response R_i' to the spatially corrected value R_{Si} at each pixel position i. Thus

$$R_{Si} = \frac{(R_W - R_B) \times (R_i' - R_{Bi})}{(R_{Wi} - R_{Bi})}, \tag{11}$$

where R_W and R_B are the mean linearized channel values for the uniform white and black (dark) samples, respectively, and R_{Wi} and R_{Bi} are the channel responses for the uniform white and black (dark) samples at each pixel location i, respectively. Similar equations were used to obtain the spatially corrected values for the green and blue channels.

C. Training and Testing Protocol
A total of 166 patches in the Macbeth ColorChecker DC chart were used as a training set for the recovery methods. Smaller training sets were derived by randomly subsampling the 166 patches to generate subtraining sets containing 120, 80, and 40 samples, and these were used to evaluate the effect of training set size on model performance for two (Maloney–Wandell and Imai–Berns) of the four recovery methods. To evaluate the generalization properties of the recovery methods, researchers in the field of camera characterization commonly use a separate test set containing samples that were not used in the

training set.[6,7,9,12,15,16] The use of such a test set guards against a model that overfits the training set and gives unrealistically good results.[7] The primary test set used in this work consisted of 50 samples from the NCS system. Figure 2 shows the colorimetric distributions of the training (Macbeth ColorChecker DC) and test (NCS) samples and, it can be observed that both are quite evenly distributed in color space. As a check on the robustness of the results for the primary test set, a second test set containing the 24 samples of the Macbeth ColorChecker chart was also used.

D. Implementation of Algorithms
The four multispectral methods were implemented in the MATLAB programming environment (Version 6.5, Release 13). The training samples were used to determine the basis functions for the linear model of reflectance that was used in each of the methods. The recovered reflectance spectra for samples in both the training and the testing sets were converted to CIE tristimulus values by use of the 1964 (10-deg) CIE observer data and the spectral power of the light source used with the camera. Color errors between measured and recovered spectra were calculated as CIELAB color-difference (ΔE_{ab}^*) values for each of the different sizes of training set (166, 120, 80, and 40 samples). When a subset of fewer than 166 training samples was used, the subset was randomly selected five times, and the mean error score was computed for the five trials. The estimated camera spectral sensitivities required for the Maloney–Wandell, Shi–Healey, and Li–Luo recovery methods were obtained from Chen[26] with methods suggested by Finlayson[27]; they are illustrated in Fig. 3.

The method for computing the basis functions for a set of reflectance spectra employs singular-value decomposition and is implemented as a single command *SVDS* in MATLAB.[28] The basis functions used were derived on the basis of the Macbeth ColorChecker DC samples in the training set and are shown in Fig. 4.
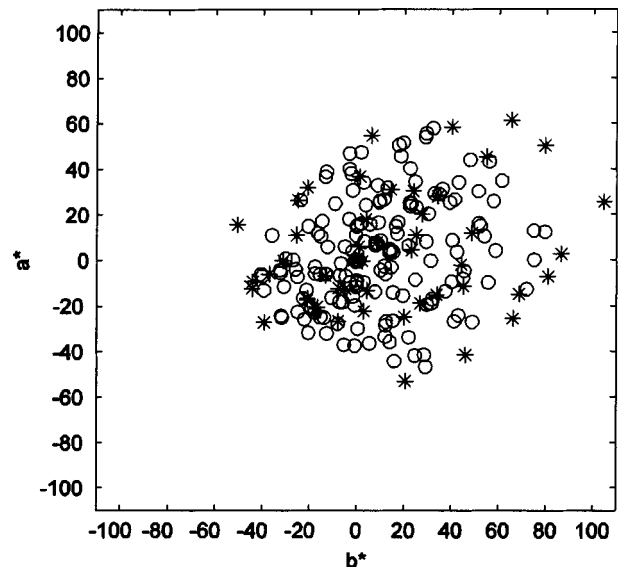

Fig. 2.   Color distributions of 166 Macbeth ColorChecker DC (circles) and 50 NCS samples (asterisks) in CIELAB a^*b^* space.
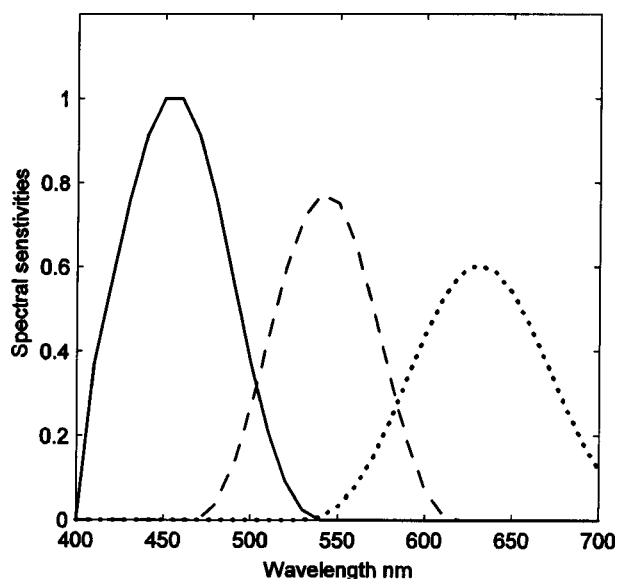
Fig. 3. Estimated camera spectral sensitivities of the blue (solid curve), green (dashed curve), and red (dotted curve) channels of the Agfa StudioCam (estimations by Chen[26]).
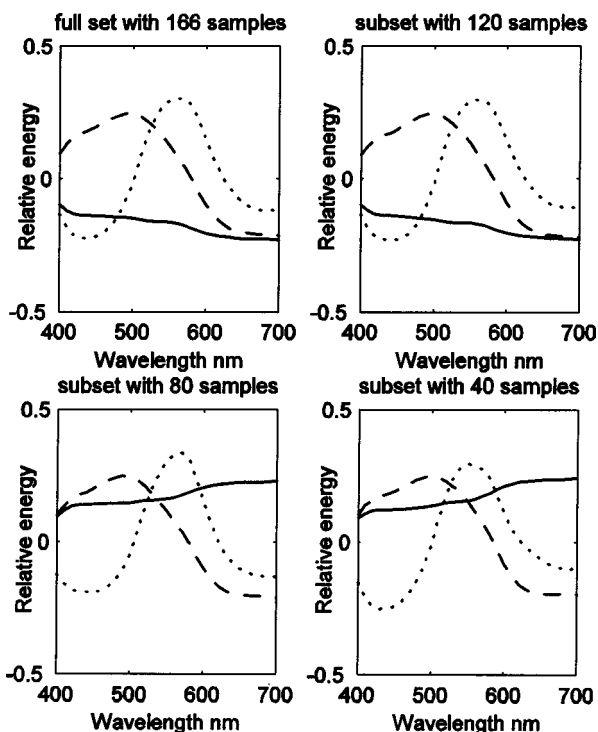

Fig. 4. First three basis functions (first component, solid curve; second component, dashed curve; third component, dotted curve) of the Macbeth ColorChecker DC training samples.

E. Statistical Test of Significance

Since distributions of color-difference values are usually skewed, a nonparametric test that makes no assumptions about the distribution of the data is preferred. The Wilcoxon matched-pairs signed-rank test is appropriate for testing populations that may differ considerably from being normally distributed. This test takes account of the magnitudes of the differences between test samples and their median.[29]

4. RESULTS

Although in principle the Maloney–Wandell and Imai–Berns methods could be used with linear models of reflectance of dimensionality greater than the number of channels (three) in the camera, recovery performance in these circumstances is poor. Results are presented in detail here only for the case of a three-dimensional linear model of reflectance. Figure 5 shows an example of reflectance-recovery performance from the Maloney–Wandell and Imai–Berns methods with a three-dimensional linear model of reflectance for one of the NCS samples (1070 R20B). In general, most of the spectra estimated with these methods are quite similar to the originals, but where errors occur they tend to be at the shorter and longer wavelengths. Since this study is concerned with colorimetric characterization, it is the colorimeteric performance, rather than spectral performance, of the methods that is of interest. For the single spectrum illustrated in Fig. 5 the colorimetric performance is 5.37 and 5.09 CIELAB ΔE units for the Maloney–Wandell and Imai–Berns methods, respectively.

Figures 6 and 7 illustrate the median color differences that result when the Maloney–Wandell and Imai–Berns methods are used for color characterization.

In both Figs. 6 and 7 it can be seen that the median errors on the training and the test sets are almost independent of the size of the training set (see also Table 1). Generally, although the median test-set errors tend to be smaller for the Imai–Berns method than for the Maloney–Wandell method, there are no statistically significant differences ($p > 0.05$).

The performances of the Shi–Healey and Li–Luo methods have been evaluated by using linear models of reflectance of dimensionality between 4 and 12. Figures 8 and 9 illustrate the recovery of reflectance for various dimensionalities of the linear models in the case of the single NCS chip that was used in Fig. 5.
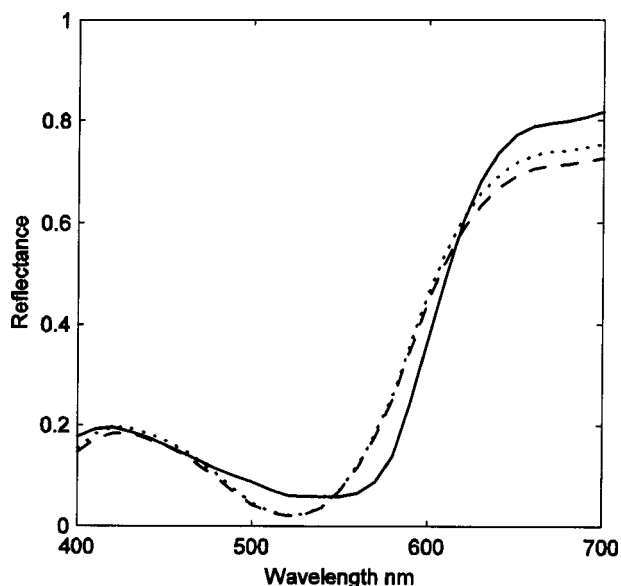

Fig. 5. Example of spectral-reflectance recovery for a NCS sample (1070 R20B, solid curve) with the Maloney-Wandell (dashed curve) and Imai–Berns (dotted curve) methods.
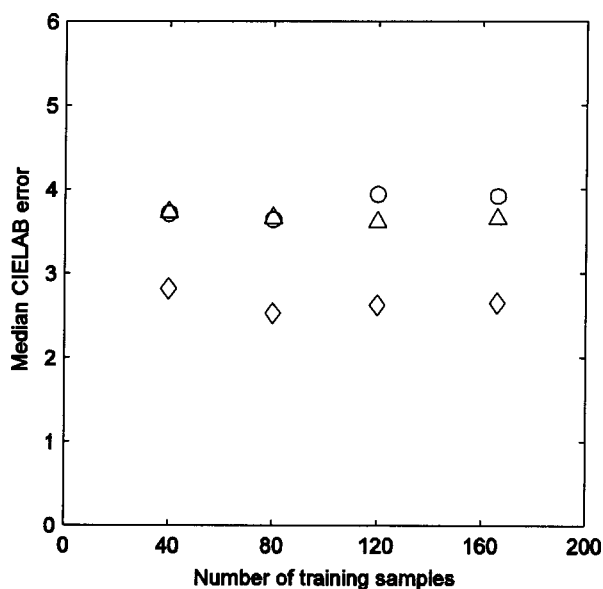
Fig. 6.   Effect of training size of the reflectance recovery with the Maloney–Wandell method. The median CIELAB errors are plotted for the training (diamonds) set and for the ColorChecker (triangles) and NCS (circles) test sets.
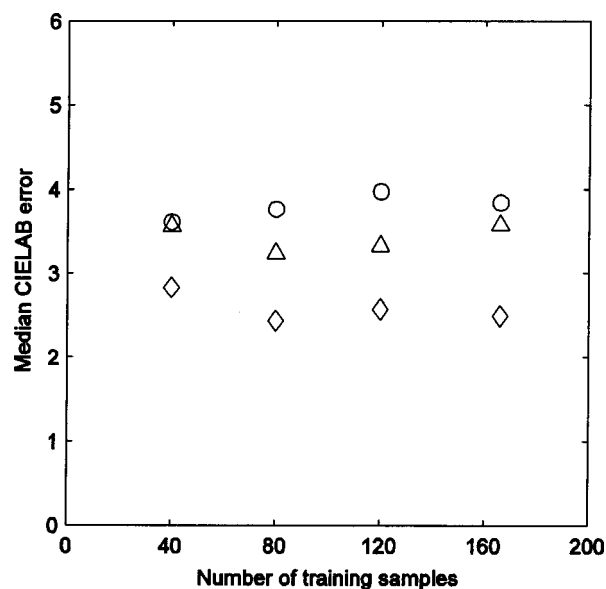

Fig. 7.   Effect of training size of the reflectance recovery with the Imai–Berns method. The median CIELAB errors are plotted for the training (diamonds) set and for the ColorChecker (triangles) and NCS (circles) test sets.

Table 1. Characterization Performance (Median CIELAB ΔE with Maximum Values in Parentheses) of Maloney–Wandell and Imai–Berns Methods for Different Training-Set Size

	Maloney–Wandell Method			Imai–Berns Method		
	Memorization (training)	Generalization (testing)		Memorization (training)	Generalization (testing)	
Number of Training Samples	DC[a]	NCS[b]	CC[c]	DC[a]	NCS[b]	CC[c]
40	2.82 (11.96)	3.71 (20.98)	3.72 (18.24)	2.83 (12.27)	3.61 (21.20)	3.56 (16.62)
80	2.53 (13.28)	3.64 (16.59)	3.66 (15.63)	2.44 (12.70)	3.76 (18.20)	3.24 (14.88)
120	2.62 (14.61)	3.94 (17.50)	3.61 (15.13)	2.57 (14.25)	3.97 (18.53)	3.33 (15.59)
166 (full set)	2.65 (14.59)	3.92 (17.30)	3.64 (15.43)	2.49 (14.18)	3.84 (17.96)	3.58 (15.28)

[a]Macbeth ColorChecker DC

[b]Natural Color System

[c]Macbeth ColorChecker

There is little evidence in Figs. 8 and 9 of any systematic effect of the dimensionality of the linear model on recovery performance for either the Shi–Healey or the Li–Luo method. However, when the performance of the Shi–Healey method on all of the samples is considered, it is evident (see Fig. 10) that the average training performance improves with the number of basis functions but the average testing performance generally deteriorates. The best generalization performance with the Shi–Healey method was found with a four-dimensional linear model. This performance (median $\Delta E = 3.79$ and 3.36 for NCS and Macbeth ColorChecker, respectively) is slightly better than the best performance (with the complete training set) of the Maloney–Wandell and Imai–Berns methods, but again the differences are not significant ($p > 0.05$).

The median errors for the Li–Luo method are illustrated in Fig. 11, and it is evident that performance deteriorates for both the training and the testing sets as the dimensionality of the linear model increases. The best performance (found with a four-dimensional linear model) of the Li–Luo model was greater than that of the other multispectral models (median $\Delta E = 3.53$ and 3.26 for NCS and Macbeth ColorChecker, respectively), but the differences were not statistically significant ($p > 0.05$). Table 2 lists the median and maximum errors for the Shi–Healey and Li–Luo methods by use of linear models of reflectance of various dimensionality and the complete training set. It can be seen that for the Shi–Healey method, even though the best average performance on the test set occurred with a four-dimensional linear model, this corre-
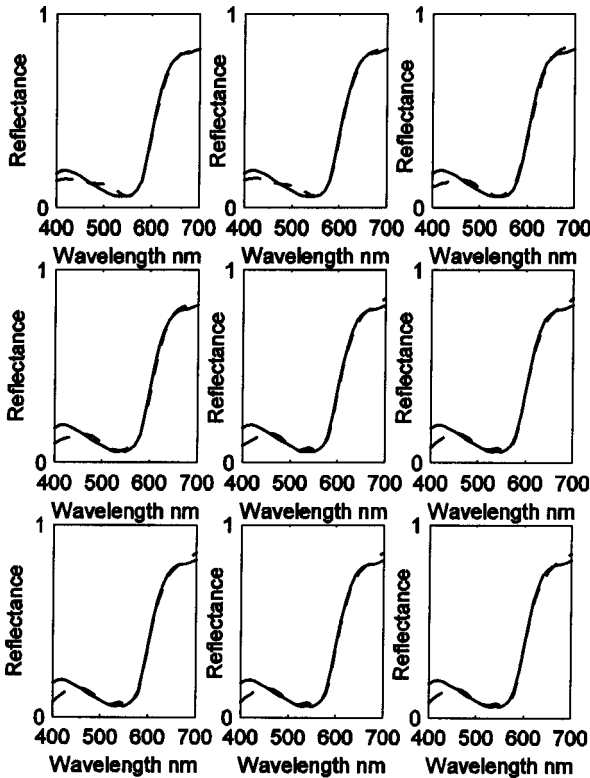
Fig. 8.   Examples of spectral-reflectance recovery for a NCS sample (1070 R20B, solid curve) by use of Shi–Healey method (dashed curve) with between 4 and 12 basis functions (estimation with 4 basis functions in top-left figure; number of basis functions increases left to right and then for each row).
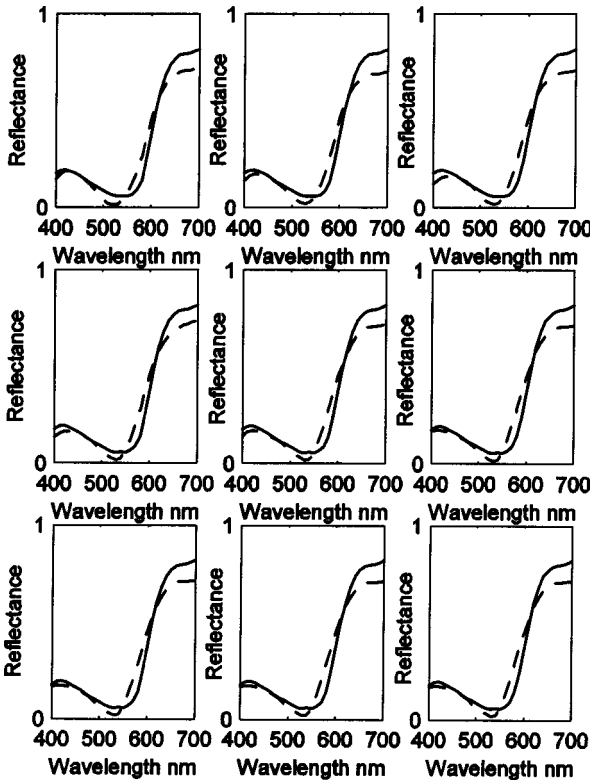

Fig. 9.   Example of spectral reflectance recovery for a NCS sample (1070 R20B, solid curve) by use of Li-Luo method (dashed curve) with between 4 and 12 basis functions (estimation with 4 basis functions in top-left figure; number of basis functions increases left to right and then for each row).

sponded to a high maximum error. Although the average performances of the four multispectral methods are statistically indistinguishable, we note that the new Li–Luo method gives the lowest maximum errors.

A previous study, using the same imaging system and data, showed that the performance of polynomial transforms and neural networks to convert directly between camera *RGB* values and CIE tristimulus values gave statistically similar results.[26] These data are reproduced for comparison as Table 3, where it can be seen that when the full training set is used, the polynomial method gives $\Delta E = 2.57$ and 2.13 and the neural network method gives

Fig. 10.   Effect of training size of the reflectance recovery with the Shi–Healey method. The median CIELAB errors are plotted for the training (diamonds) set and for the ColorChecker (triangles) and NCS (circles) test sets.
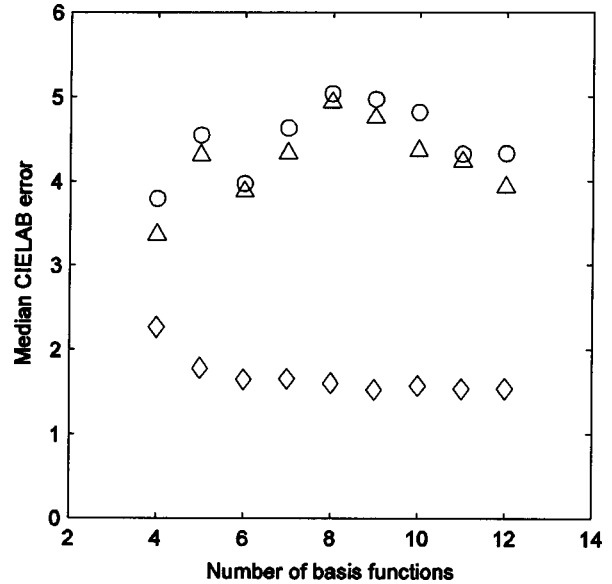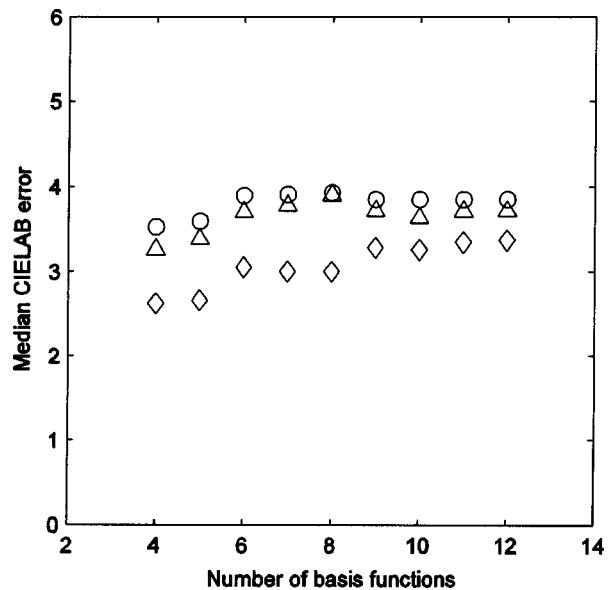

Fig. 11.   Effect of training size of the reflectance recovery with the Li–Luo method. The median CIELAB errors are plotted for the training (diamonds) set and for the ColorChecker (triangles) and NCS (circles) test sets.

Table 2. Characterization Performance (Median CIELAB ΔE with Maximum Values in Parentheses) of Shi–Healey and Li–Luo Methods with Different Numbers of Basis Functions[a]

Number of Basis Functions	Shi–Healey Method			Li–Luo Method		
	Memorization (training)	Generalization (testing)		Memorization (training)	Generalization (testing)	
	DC	NCS	CC	DC	NCS	CC
4	2.27	3.79	3.36	2.63	3.53	3.26
	(12.38)	(23.39)	(20.14)	(10.66)	(14.87)	(12.95)
5	1.78	4.55	4.31	2.66	3.59	3.39
	(8.91)	(14.38)	(17.12)	(11.37)	(15.14)	(13.72)
6	1.65	3.97	3.88	3.05	3.90	3.70
	(8.93)	(15.92)	(14.58)	(11.99)	(16.11)	(14.14)
7	1.66	4.63	4.33	3.00	3.91	3.78
	(8.93)	(19.44)	(18.82)	(11.72)	(16.00)	(15.13)
8	1.61	5.04	4.93	3.00	3.93	3.90
	(8.92)	(21.31)	(19.29)	(11.71)	(16.00)	(15.27)
9	1.53	4.97	4.75	3.28	3.85	3.72
	(8.99)	(19.46)	(19.17)	(13.10)	(16.80)	(15.12)
10	1.58	4.82	4.36	3.26	3.85	3.63
	(6.48)	(17.70)	(19.07)	(13.13)	(16.81)	(14.06)
11	1.54	4.32	4.23	3.35	3.85	3.71
	(6.55)	(14.64)	(15.65)	(13.62)	(17.01)	(14.38)
12	1.54	4.33	3.93	3.37	3.85	3.71
	(6.58)	(14.56)	(15.26)	(13.66)	(17.03)	(14.53)

[a]DC, NCS, and CC as defined in Table 1.

Table 3. Characterization Performance (Median CIELAB ΔE with Maximum Values in Parentheses) Using the Best Polynomial (3×20 Model) and Neural Networks (18 Hidden Units) Methods for Different Training-Set Sizes[a]

Number of Training Samples	Polynomial			Neural networks		
	Memorization (training)	Generalization (testing)		Memorization (training)	Generalization (testing)	
	DC	NCS	CC	DC	NCS	CC
40	1.13	3.98	3.55	1.24	7.46	4.55
	(4.34)	(47.30)	(14.74)	(4.22)	(49.42)	(14.00)
80	1.23	2.74	2.60	1.23	4.37	2.43
	(5.59)	(16.71)	(11.90)	(6.02)	(20.19)	(11.36)
120	1.39	2.68	2.40	1.39	3.19	2.41
	(6.81)	(13.87)	(10.93)	(6.40)	(16.16)	(11.99)
166 (full set)	1.39	2.57	2.13	1.53	2.89	2.18
	(7.56)	(15.04)	(10.65)	(8.12)	(16.66)	(11.30)

[a]DC, NCS, and CC as defined in Table 1.

$\Delta E = 2.89$ and 2.18 for the NCS and the Macbeth ColorChecker test sets, respectively. The performance of these conventional methods is significantly better than the results obtained with the multispectral methods ($p < 0.05$ for comparison with each of the multispectral methods).

5. DISCUSSION

In this study four multispectral reflectance-recovery methods were evaluated in terms of camera characterization for one high-quality imaging system and three sets of data (a training set and two test sets). The generalization performance (median ΔE) of the techniques for the NSC

test set with the full set of training samples was found to be 3.84, 3.92, 3.79, and 3.53, respectively, for the Imai–Berns method (with three basis functions), the Maloney–Wandell method (with three basis functions), the Shi–Healey method (with four basis functions), and the Li–Luo method (with four basis functions). The generalization performance (median ΔE) of the techniques for the Macbeth ColorChecker test set with the full set of training samples was found to be 3.64, 3.58, 3.36, and 3.26.

We note that for the Maloney–Wandell recovery method the performance may be limited by the accuracy to which the spectral sensitivities of the channels of the camera were estimated. Given, however, that the Imai–Berns

method finds the least-squares linear transform between the representation of the spectra in the linear model and the camera responses to those spectra, it seems unlikely that the Maloney–Wandell method would outperform the Imai–Berns method.

In a related study using the same imaging system, we found that polynomial and neural-network methods are able to perform characterization on the same experimental data with a median CIELAB ΔE of 2.57 and 2.89, respectively, for the NCS samples and 2.13 and 2.18, respectively, for the ColorChecker samples.[16] We find no evidence, therefore, that multispectral-imaging techniques provide any advantage over conventional characterization methods for a three-channel camera imaging under a single illuminant. Further work is required to evaluate multispectral techniques for multiple imaging under more than one light source and for cameras with more than three color channels.

6. CONCLUSIONS

In this study a new reflectance-recovery technique has been introduced that has been shown to outperform three existing recovery methods in terms of colorimetric accuracy. The Li–Luo technique uses a high-dimensional linear model of reflectance. For an m-dimensional model (where $m > 3$), $m - 3$ degrees of freedom are optimized to find the smoothest reflectance consistent with a set of three camera response values. Since the purpose of this study was to investigate whether reflectance-recovery techniques may be useful for camera characterization, the recovery techniques were evaluated by using a colorimetric measure. The new method was found to give the best performance in these terms. For other applications, however, it may be more important to assess the degree of spectral accuracy of the recovery techniques, and it is by no means certain that the best algorithm in colorimetric terms will be the best method in spectral terms. For spectral-based applications it may be necessary to ascertain the true dimensionality of the spectral reflectance of the surfaces.[30] Although the validity of using spectral-recovery methods for device characterization has been established by this work and elsewhere,[15] a related study using the same camera and data as reported in this study has shown that none of the four recovery techniques that were evaluated could outperform more standard polynomial techniques.[16]

The corresponding author's e-mail address is s.westland@leeds.ac.uk.

REFERENCES

1. B. A. Wandell and J. E. Farrell, "Water into wine: converting scanner RGB to tristimulus XYZ," in "Device-independent color image and imaging systems integration," R. J. Motta and H. A. Berberian, eds., Proc. SPIE **1909**, 92–101 (1993).
2. J. E. Farrell, D. Sherman, and B. A. Wandell, "How to turn your scanner into a colorimeter," in *Proceedings of the 10th International Conference on Advances in Non-impact Printing Technologies* (Society for Imaging Science and Technology, Springfield, Va., 1994).
3. W. Wu, J. P. Allebach, and M. Analoui, "Imaging colorimetry using a digital camera," J. Imaging Sci. Technol. **44**, 267–279 (2000).
4. T. Johnson, "Methods for characterising color scanners and digital cameras," Displays **16**, 183–191 (1996).
5. G. D. Finlayson and P. M. Morovic, "Metamer constrained color correction," in *Proceedings of the 7th Color Imaging Science Conference* (Society for Imaging Science and Technology, Springfield, Va., 1999).
6. G. Hong, M. R. Luo, and P. A. Rhodes, "A study of digital camera colorimetric characterization based on polynomial modelling," Color Res. Appl. **26**, 76–84 (2001).
7. S. Westland and C. Ripamonti, *Computational Colour Science: Using MATLAB* (Wiley, Chichester, UK, 2004).
8. F. H. Imai, S Quan, M. R. Rosen, and R. S. Berns, "Digital camera filter design for colorimetric and spectral accuracy," in *Proceedings of the 3rd International Conference on Multispectral Color Science* (Joensuu, Finland), 23–26 (2001).
9. J. Y. Hardeberg, "Acquisition and reproduction of colour images: colorimetric and multispectral approaches," Ph.D. thesis (Ecole Nationale Supérieure des Télécommunications, Paris, 1999).
10. H. Sugiura, T. Kuno, N. Watanabe, N. Matoba, J. Hayashi, and Y. Miyake, "Development of highly accurate multispectral cameras," in *Proceedings of the International Symposium on Multispectral Imaging and Color Reproduction for Digital Archives* (Society of Multispectral Imaging of Japan, Chiba, Japan 1999).
11. D. Connah, S. Westland, and M. G. A. Thomson, "Recovering spectral information using digital camera systems," Coloration Technol **117**, 309–312 (2001).
12. H. -L. Shen and J. H. Xin, "Spectral characterization of a color scanner by adaptive estimation," J. Opt. Soc. Am. A **21**, 1125–1130 (2004).
13. L. T. Maloney, "Evaluation of linear models of surface spectral reflectance with small numbers of parameters," J. Opt. Soc. Am. A **3**, 1673–1683 (1986).
14. R. S. Berns and M. J. Shyu, "Colorimetric characterization of a desktop drum scanner using a spectral model," J. Electron. Imaging **4**, 360–372 (1995).
15. M. Shi and G. Healey, "Using reflectance models for color scanner calibration," J. Opt. Soc. Am. A **19**, 645–656 (2002).
16. V. Cheung, S. Westland, D. Connah, and C. Ripamonti, "A comparative study of characterization of color cameras using neural networks and polynomial transforms," Coloration Technol **120**, 19–25 (2004).
17. L. T. Maloney and B. A. Wandell, "Color constancy: a method for recovering surface spectral reflectance," J. Opt. Soc. Am. A **3**, 29–33 (1986).
18. F. H. Imai and R. S. Berns, "Spectral estimation using trichromatic digital cameras," in *Proceedings of the International Symposium on Multispectral Imaging and Color Reproduction for Digital Archives* (Society of Multispectral Imaging of Japan, Chiba, Japan, 1999).
19. C. J. Li and M. R. Luo, "The estimation of spectral reflectances using the smoothness constraint condition," in *Proceedings of the 9th Color Imaging Science Conference* (Society for Imaging Science and Technology, Springfield, Va., 2001).
20. C. van Trigt, "Smoothest reflectance functions I: definition and main results," J. Opt. Soc. Am. A **7**, 1891–1904 (1990).
21. C. van Trigt, "Smoothest reflectance functions II: complete results," J. Opt. Soc. Am. A **7**, 2208–2222 (1990).
22. P. Morovič, "Metamer sets," Ph.D. thesis, (University of East Anglia, Norwich, UK, 2002).
23. M. G. A. Thomson and S. Westland, "Color-imager calibration by parametric fitting of sensor responses," Color Res. Appl. **26**, 442–449 (2001).
24. V. Cheung, S. Westland, and M. G. A. Thomson, "Accurate estimation of the non-linearity of input-output response for color cameras," Color Res. Appl. **29**, 406–412 (2004).
25. Q. Sun and M. D. Fairchild, "Statistical characterization of spectral reflectances in human portraiture," *Proceedings of the 9th Color Imaging Science Conference* (Society

for Imaging Science and Technology, Springfield, Va., 2001).

26. Q. Chen, "Estimation of digital camera's spectral sensitivity," M.Sc. dissertation, (University of Derby, Derby, UK 2001).

27. G. D. Finlayson, S. D. Hordley, and P. M. Hubel, "Recovering device sensitivities with quadratic programming," in *Proceedings of the 6th Color Imaging Science Conference* (Society for Imaging Science and

Technology, Springfield, Va., 1998).

28. G. J. Borse, *Numerical Methods with MATLAB: A Resource for Scientists and Engineers* (PWS, London, 1997).

29. G. Upton and I. Cook, *Understanding Statistics* (Oxford U. Press, Oxford, UK, 1996).

30. J. Y. Hardeberg, "On the spectral dimensionality of object colors," in *Proceedings of the 1st European Conference on Color in Graphics, Image and Vision* (Society for Imaging Science and Technology, Springfield, Va., 2002).